2010

Robust fuzzy control of an active magnetic bearing subject to voltage saturation

Haiping Du
University of Technology, Sydney, hdu@uow.edu.au

Nong Zhang
University of Technology, Sydney

Jinchen Ji
University of Technology, Sydney

Wei Gao
Ludong University, China,Shanghai Jiao Tong University, wgao@uow.edu.au

Robust fuzzy control of an active magnetic bearing subject to voltage saturation

Abstract

Based on a recently proposed model for the active-magnetic-bearing (AMB) switching mode of operation, this paper presents a robust Takagi-Sugeno-model-based fuzzy-control strategy to stabilize the AMB with fast response speed subject to control-voltage saturation and parameter uncertainties. The sufficient conditions for the existence of such a controller are derived in terms of linear matrix inequalities. Numerical simulations against the proposed AMB model and a high-fidelity AMB model are used to validate the effectiveness of the proposed approach.

Disciplines

Physical Sciences and Mathematics

Publication Details

H. Du, N. Zhang, J. C. Ji & W. Gao, "Robust fuzzy control of an active magnetic bearing subject to voltage saturation," IEEE transactions on control systems technology : a publication of the IEEE Control Systems Technology, 18 (1), pp. 164-169, 2010.

Robust Fuzzy Control of an Active Magnetic Bearing Subject to Voltage Saturation

Haiping Du, Nong Zhang, J. C. Ji, and Wei Gao

***Abstract*—Based on a recently proposed model for the active-magnetic-bearing (AMB) switching mode of operation, this paper presents a robust Takagi–Sugeno-model-based fuzzy-control strategy to stabilize the AMB with fast response speed subject to control-voltage saturation and parameter uncertainties. The sufficient conditions for the existence of such a controller are derived in terms of linear matrix inequalities. Numerical simulations against the proposed AMB model and a high-fidelity AMB model are used to validate the effectiveness of the proposed approach.**

***Index Terms*—Input saturation, magnetic levitation, nonlinear system, robust control, T-S fuzzy model.**

I. Introduction

ACTIVE MAGNETIC bearings (AMBs) are being increasingly used in a variety of rotating machines, e.g., artificial heart pumps, compressors, high-speed milling spindles, flywheel energy-storage systems, etc. With the noncontact nature, AMBs offer many appealing advantages over conventional mechanical bearings, such as low power loss, elimination of oil supply and lubrication, long life, low weight, etc.

Since AMBs are open-loop unstable systems, they require feedback control for stable operation. On the other hand, in order to reduce electromagnetic losses in an AMB system due to eddy current or ohmic effects, it is desirable to reduce or eliminate the bias current during AMB operation, which, however, enhances the AMB-system nonlinearities and may lead to a control saturation or singularity. Due to these conflicting objectives, the design of stabilizing control laws for low-loss AMBs subject to saturation constraints is, thus, a challenging problem [1]–[5]. In this paper, we consider the control of AMBs operating in the switching mode with the constraint on the control-voltage amplitude. This problem was previously addressed in [3] using the passivation, small-gain, and nested-saturation designs. In addition, a forwarding-like approach was recently presented to construct a stabilizing controller [4] for the same AMB model used in [3] and [8]. It is noted that the control laws proposed in [3] and [4], see [3, eqs. (22) and (38)] and [4, (30)] for instance, require the accurate knowledge of the parameters ϵ, β_0, and β_1, where $\epsilon = \bar{\Phi}_0/\Phi_{\rm sat}$, $\Phi_{\rm sat}$ is the value of the saturation (maximum) flux and $\bar{\Phi}_0$, β_0, and β_1 are parameters that are defined in terms of bias flux, initial control flux, rotor mass, etc., and will be given in the next section. Thus, it is possible that these control laws may be prone to uncertainties in the AMB model parameters like bias flux, initial control flux, rotor mass, and so on. Robustness to parameter uncertainties may be less of an issue for stabilization/regulation problems of an AMB, but model uncertainty could be a major obstacle that requires more close attention in tracking and disturbance-rejection problems [1]. In this paper, we present a new approach to stabilize the AMB model of [3] with the consideration of the parameter uncertainties into controller design process. Namely, we use Takagi–Sugeno (T-S) fuzzy-control method [6] to design a robust control law that renders the AMB system globally asymptotically stable to the origin. At the same time, a decay rate is considered as a control performance specification for achieving fast response speed to the AMB-system state trajectories. Although not presented in this paper, the control law to be developed can be easily modified to account for the disturbance-rejection problem.

The rest of this paper is organized as follows. Section 2 presents the AMB model. The T-S fuzzy model of the nonlinear uncertain AMB model is given in Section 3. In Section 4, the computational algorithm for the fuzzy state-feedback controller is provided. Section 5 presents the design results and simulations. Finally, we summarize our findings in Section 6.

The notation used throughout this paper is fairly standard. For a real symmetric matrix W, the notation of $W > 0 (W < 0)$ is used to denote its positive (negative) definiteness. I is used to denote the identity matrix of appropriate dimensions. To simplify notation, $*$ is used to represent a block matrix which is readily inferred by symmetry.

II. AMB Model

A simplified 1-DOF AMB system, as shown in Fig. 1, is studied in this paper. This model has been used in [1], [3], and [4] for low- and zero-bias control designs for AMBs. Neglecting gravity, the mechanical subsystem of the AMB model is governed by

$$m\ddot{z}(t) = F_1(t) - F_2(t) \tag{1}$$

where m is the rotor mass, $z(t)$ represents the position of the rotor center, and $F_1(t)$ and $F_2(t)$ denote the forces produced by the two electromagnets, given by

$$F_i(t) = \frac{\Phi_i^2(t)}{\mu_0 A_g}, \qquad i = 1, 2 \tag{2}$$

where μ_0 is the permeability of air, A_g is the cross-sectional area of the electromagnet, and $\Phi_i(t)$ is the total magnetic flux of the ith electromagnet. In nonzero-bias operation, the total magnetic

Manuscript received January 08, 2008; revised July 22, 2008. Manuscript received in final form November 12, 2008. First published April 17, 2009; current version published December 23, 2009. Recommended by Associate Editor C. Knopse. This work was supported in part by the University of Technology, Sydney, under the Early Career Research Grant and by the Australian Research Council's Discovery Projects funding scheme under Project DP0773415.

The authors are with the Mechatronics and Intelligent Systems, Faculty of Engineering, University of Technology, Sydney, Broadway, N.S.W. 2007, Australia (e-mail: hdu@eng.uts.edu.au; nong.zhang@uts.edu.au; jinchen.ji@uts.edu.au; wei.gao@uts.edu.au).

Digital Object Identifier 10.1109/TCST.2008.2009644

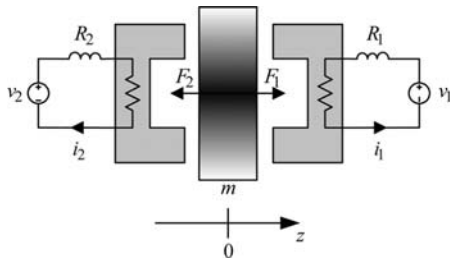

Fig. 1. Schematic diagram of a simplified 1-DOF AMB system.

flux $\Phi_i(t)$ is composed of the bias flux Φ_0 and the perturbation (control) flux $\phi_i(t)$ which is generated by the ith electromagnet. The total flux generated by the ith electromagnet is therefore

$$\Phi_i(t) = \Phi_0 + \phi_i(t), \qquad i = 1, 2. \tag{3}$$

The electrical dynamics are given by

$$\dot{\Phi}_i(t) = \dot{\phi}_i(t) = \frac{v_i(t)}{N}, \qquad i = 1, 2 \tag{4}$$

where N denotes the number of coil turns in the electromagnet and v_i is the input control voltage of the ith electromagnet. The coil resistance R_i was neglected here for simplicity.

In this paper, we also use the new form proposed in [1] and [3] for the AMB dynamics in the switching mode of operation. The details and justification of the model derivation can be found in [1].

Let the generalized control flux be defined as

$$\phi(t) = \phi_1(t) - \phi_2(t) \tag{5}$$

and consider the voltage switching strategy

$$\begin{aligned} &v_1(t) = v(t) \quad v_2(t) = 0, \qquad \text{when } \phi(t) \geq 0 \\ &v_1(t) = 0 \quad v_2(t) = -v(t), \qquad \text{when } \phi(t) < 0 \end{aligned} \tag{6}$$

where $v(t)$ is the generalized control voltage. Then, from (1), (2), (3), (4), (5), and (6), the AMB model has the equivalent form

$$\ddot{z}(t) = \frac{1}{m\mu_0 A_g}\left(2\bar{\Phi}_0\phi(t) + \phi(t)|\phi(t)|\right) \tag{7}$$

where $\bar{\Phi}_0 = \Phi_0 + \min\{\phi_1(0), \phi_2(0)\}$.

Defining the state variables $x_1(t) = z(t)$, $x_2(t) = \dot{z}(t)$, and $x_3(t) = \phi(t)$ and the change of control variable $v(t) = u(t)$ and considering that the input voltage to the original AMB model is amplitude-limited, the state-space equation of the nonlinear time-varying AMB model can be written as

$$\dot{x}(t) = A(t)x(t) + B\bar{u}(t) \tag{8}$$

where $x(t) = [x_1(t) \quad x_2(t) \quad x_3(t)]^{\mathrm{T}}$ is the state vector and $\bar{u}(t)$ is the bounded input voltage to the AMB model. In a real application, the input voltage is bounded as $\bar{u}(t) = \mathrm{sat}(u(t))$, where $\mathrm{sat}(u(t))$ is a saturation function of control input $u(t)$ and is defined as

$$\mathrm{sat}(u(t)) = \begin{cases} -u_{\lim}, & \text{if } u(t) < -u_{\lim} \\ u(t), & \text{if } -u_{\lim} \leq u(t) \leq u_{\lim} \\ u_{\lim}, & \text{if } u(t) > u_{\lim} \end{cases} \tag{9}$$

where $u_{\lim}$ is a control input limit, and $u_{\lim} = v_{\max}$, where $v_{\max}$ is the maximum voltage limit. The matrices are given as

$$\begin{aligned} A(t) &= \begin{bmatrix} 0 & 1 & 0 \\ 0 & 0 & \beta_0 + \beta_1 f(\phi(t)) \\ 0 & 0 & 0 \end{bmatrix} \\ B &= \begin{bmatrix} 0 \\ 0 \\ 1/N \end{bmatrix} \end{aligned} \tag{10}$$

where $\beta_0 = (2\bar{\Phi}_0)/(m\mu_0 A_g$ and $\beta_1 = (1)/(m\mu_0 A_g)$ and $f(\phi(t))$ is a nonlinear function given as

$$f(\phi(t)) = |\phi(t)|. \tag{11}$$

III. T-S Fuzzy Model of AMB

Consider the magnetic-material saturation in practice [7], the generalized control flux $\phi(t)(x_3(t))$ will be bounded by its minimum value $\phi_{\min}$ and its maximum value $\phi_{\max}$, and hence, the nonlinear function $f(\phi(t))$ in (10) will be bounded by its minimum value $f_{\min}$ and its maximum value $f_{\max}$. Using the idea of "sector nonlinearity" [6], the nonlinear function $f(\phi(t))$ can be represented by

$$f(\phi(t)) = M_1(\xi(t))\, f_{\max} + M_2(\xi(t))\, f_{\min} \tag{12}$$

where $\xi(t) = f(\phi(t))$ is the premise variable, $M_1(\xi(t))$ and $M_2(\xi(t))$ are membership functions, and

$$\begin{aligned} M_1(\xi(t)) &= \frac{f(\phi(t)) - f_{\min}}{f_{\max} - f_{\min}} \\ M_2(\xi(t)) &= \frac{f_{\max} - f(\phi(t))}{f_{\max} - f_{\min}}. \end{aligned} \tag{13}$$

Then, under the assumption on bounds of the generalized control flux $\phi(t) \in [\phi_{\min}, \phi_{\max}]$, we can exactly represent the nonlinear time-varying AMB model (8) with the T-S fuzzy model as

$$\dot{x}(t) = \sum_{i=1}^{2} h_i(\xi(t))A_i x(t) + B\bar{u}(t) \tag{14}$$

where A_1 and A_2 are matrices that are obtained by replacing $f(\phi(t))$ in matrix $A(t)$ with $f_{\max}$ and $f_{\min}$, respectively, and

$$\begin{aligned} h_i(\xi(t)) &= M_i(\xi(t)) \\ h_i(\xi(t)) &\geq 0, \qquad i = 1, 2 \\ \sum_{i=1}^{2} h_i(\xi(t)) &= 1. \end{aligned}$$

Since the generalized control flux $\phi(t)(x_3(t))$ can be measured or estimated [3], the premise variable $\xi(t)$ can be obtained, and the T-S fuzzy model (14) can be constructed.

It is noted from (10) that the parameters β_0 and β_1 are dependent on the bias flux, the initial conditions of the perturbation (control) flux, and the rotor mass, of which values are most likely to be uncertain; therefore, the parameter uncertainties should be considered so that the AMB model is expressed as

$$\dot{x}(t) = \sum_{i=1}^{2} h_i\left(\xi(t)\right)\left(A_i + \Delta A_i\right)x(t) + B\bar{u}(t) \tag{15}$$

where $\Delta A_i = HFE_i$ represents the parameter uncertainties, H and E_i are known constant matrices with appropriate dimensions, and F is an unknown matrix function bounded by $F^{\mathrm{T}}F \leq I$.

In order to avoid the large number of inequality problems when the input saturation constraint is characterized in terms of convex hull of some linear combinations of linear and saturation functions [8], a norm-bounded approach is used to handle the saturation nonlinearity. Hence, the (15) will be written as

$$\begin{aligned}\dot{x}(t) &= \sum_{i=1}^{2} h_i(\xi(t))(A_i + \Delta A_i)x(t) + B\bar{u}(t) \\ &= \sum_{i=1}^{2} h_i(\xi(t))(A_i + \Delta A_i)x(t) \\ &\quad + B\frac{1+\varepsilon}{2}u(t) + B\left(\bar{u}(t) - \frac{1+\varepsilon}{2}u(t)\right) \\ &= (A_h + \Delta A_h)x(t) + B\frac{1+\varepsilon}{2}u(t) \\ &\quad + B\left(\bar{u}(t) - \frac{1+\varepsilon}{2}u(t)\right)\end{aligned} \tag{16}$$

where $A_h = \sum_{i=1}^{2} h_i(\xi(t))A_i$, $\Delta A_h = \sum_{i=1}^{2} h_i(\xi(t))$, and $\Delta A_i = \sum_{i=1}^{2} h_i(\xi(t))HFE_i = HFE_h$, $0 < \varepsilon < 1$. Moreover, we have the following lemma.

Lemma 1: [9] For the saturation constraint defined by (9), as long as $|u(t)| \leq (u_{\lim})/(\varepsilon)$, we have

$$\left\|\bar{u}(t) - \frac{1+\varepsilon}{2}u(t)\right\| \leq \frac{1-\varepsilon}{2}\left\|u(t)\right\| \tag{17}$$

and hence

$$\left[\bar{u}(t) - \frac{1+\varepsilon}{2}u(t)\right]^{\mathrm{T}}\left[\bar{u}(t) - \frac{1+\varepsilon}{2}u(t)\right] \leq \left(\frac{1-\varepsilon}{2}\right)^2 u^{\mathrm{T}}(t)u(t) \tag{18}$$

where $0 < \varepsilon < 1$.

IV. Robust Fuzzy-Controller Design

Our goal in this paper is to design a robust fuzzy feedback control law based on the so-called parallel-distributed compensation (PDC) scheme [6] as

$$u(t) = \sum_{i=1}^{2} h_i\left(\xi(t)\right)K_i x(t) = K_h x(t) \tag{19}$$

where $K_h = \sum_{i=1}^{2} h_i(\xi(t))K_i, K_i$ is the state-feedback gain matrix to be designed, such that the equilibrium of the T-S fuzzy system (16) with controller (19) is globally asymptotically stable (quadratically) stable with a decay rate $\alpha > 0$. Note that the decay rate (or the largest Lyapunov exponent) is related to the transient performances on speed of response and overshoot and indicates the convergence rate of the trajectories.

To design the controller, the following lemma will be used.

Lemma 2: For any matrices (or vectors) X and Y with appropriate dimensions, we have

$$X^{\mathrm{T}}Y + Y^{\mathrm{T}}X \leq \epsilon X^{\mathrm{T}}X + \epsilon^{-1}Y^{\mathrm{T}}Y$$

where $\epsilon > 0$ is any scalar.

Theorem 1: For given scalars $0 < \varepsilon < 1$, $\rho > 0$, and $\alpha > 0$, matrices H and $E_i, i = 1, 2$, the equilibrium of the T-S fuzzy system (16) with controller (19) is globally asymptotically stable (quadratically) stable with a decay rate α if there exist matrix $Q > 0$, matrices $Y_i, i = 1, 2$, scalars $\epsilon_1 > 0$ and $\epsilon_2 > 0$ such that

$$\begin{bmatrix} QA_i^{\mathrm{T}} + A_iQ + \frac{1+\varepsilon}{2}\left[Y_i^{\mathrm{T}}B^{\mathrm{T}} + BY_i\right] & Y_i^{\mathrm{T}} & QE_i^{\mathrm{T}} \\ \quad + \epsilon_1^{-1}BB^{\mathrm{T}} + \epsilon_2^{-1}HH^{\mathrm{T}} + 2\alpha Q & & \\ * & -\epsilon_1^{-1}\left(\frac{2}{1-\varepsilon}\right)^2 I & 0 \\ * & * & -\epsilon_2^{-1}I \end{bmatrix} < 0 \tag{20}$$

$$\begin{bmatrix} \left(\frac{u_{\lim}}{\varepsilon}\right)^2 & Y_i \\ Y_i^{\mathrm{T}} & \rho^{-1}Q \end{bmatrix} \geq 0. \tag{21}$$

Moreover, the robust fuzzy state-feedback gains can be obtained as $K_i = Y_iQ^{-1}, i = 1, 2$.

Proof: Let us define a quadratic Lyapunov function for the system (16) as

$$V\left(x(t)\right) = x^{\mathrm{T}}(t)Px(t) \tag{22}$$

where P is a positive-definite matrix.

By differentiating (22), we obtain

$$\begin{aligned}\dot{V}(x(t)) &= \dot{x}^{\mathrm{T}}(t)Px(t) + x^{\mathrm{T}}(t)P\dot{x}(t) \\ &= \left[(A_h + \Delta A_h)x(t) + B\bar{u}(t)\right]^{\mathrm{T}}Px(t) \\ &\quad + x^{\mathrm{T}}(t)P\left[(A_h + \Delta A_h)x(t) + B\bar{u}(t)\right] \\ &= \left[(A_h + \Delta A_h)x(t) + B\frac{1+\varepsilon}{2}u(t)\right. \\ &\qquad \left. + B\left(\bar{u}(t) - \frac{1+\varepsilon}{2}u(t)\right)\right]^{\mathrm{T}}Px(t) \\ &\quad + x^{\mathrm{T}}(t)P\left[(A_h + \Delta A_h)x(t) + B\frac{1+\varepsilon}{2}u(t)\right. \\ &\qquad \left. + B\left(\bar{u}(t) - \frac{1+\varepsilon}{2}u(t)\right)\right].\end{aligned} \tag{23}$$

By Lemmas 1 and 2 and (19), we have the expression for $\dot{V}(x(t))$, shown at the bottom of the next page. Furthermore,

we require (24), shown at the bottom of the page, where the positive number α is the decay rate. It can be inferred from (24) that if we have (25), shown at the bottom of the page, then $\dot{V}(x(t)) \leq -2\alpha V(x(t))$. Moreover, the fuzzy system (16) with the controller (19) is quadratically stable with decay rate α.

Pre- and postmultiplying (25) by P^{-1} and its transpose, respectively, and defining $Q = P^{-1}$ and $Y_h = K_h P^{-1}$, the condition $\Pi < 0$ is equivalent to (26), shown at the bottom of the page. By the Schur complement, $\Sigma < 0$ is equivalent to (27), shown at the bottom of the page. By the definitions $A_h = \sum_{i=1}^{2} h_i(\xi(t))A_i$, $Y_h = \sum_{i=1}^{2} h_i(\xi(t))Y_i$, and $E_h = \sum_{i=1}^{2} h_i(\xi(t))E_i$ and the fact that $h_i(\xi(t)) \geq 0$ and $\sum_{i=1}^{2} h_i(\xi(t)) = 1$, $\Theta < 0$ is equivalent to (20).

On the other hand, from (19), the constraint $|u(t)| \leq (u_{\lim})/(\varepsilon)$ can be expressed as

$$\left| \sum_{i=1}^{2} h_i(\xi(t)) K_i x(t) \right| \leq \frac{u_{\lim}}{\varepsilon}. \tag{28}$$

It is obvious that if $|K_i x(t)| \leq (u_{\lim})/(\varepsilon)$, then (28) holds. Let $\Omega(K) = \{x(t) || x^{\mathrm{T}}(t) K_i^{\mathrm{T}} K_i x(t)| \leq ((u_{\lim})/(\varepsilon))^2\}$, the equivalent condition for an ellipsoid $\Omega(P,\rho) = \{x(t) | x^{\mathrm{T}}(t) P x(t) \leq \rho\}$ being a subset of $\Omega(K)$, i.e., $\Omega(P,\rho) \subset \Omega(K)$, is [8]

$$K_i \left(\frac{P}{\rho}\right)^{-1} K_i^{\mathrm{T}} \leq \left(\frac{u_{\lim}}{\varepsilon}\right)^2. \tag{29}$$

By Schur complement, inequality (29) can be written as

$$\begin{bmatrix} \left(\frac{u_{\lim}}{\varepsilon}\right)^2 & K_i \left(\frac{P}{\rho}\right)^{-1} \\ \left(\frac{P}{\rho}\right)^{-1} K_i^{\mathrm{T}} & \left(\frac{P}{\rho}\right)^{-1} \end{bmatrix} \geq 0. \tag{30}$$

Using the definitions $Q = P^{-1}$ and $Y_i = K_i Q$, inequality (30) is equivalent to (21). This completes the proof. □

V. Numerical Example

Similar to the work in [3] and [4], in this section, we validate the previous theoretical results through numerical simulations on both the AMB model (10), which is used for the control-law design, and the same high-fidelity model of 1-DOF magnetic-levitation system [7], [10] used in [3] and [4]. The high-fidelity

$$\begin{aligned} \dot{V}(x(t)) &\leq x^{\mathrm{T}}(t) \left[A_h^{\mathrm{T}} P + P A_h + \Delta A_h^{\mathrm{T}} P + P \Delta A_h + \left(B \frac{1+\varepsilon}{2} K_h \right)^{\mathrm{T}} P + P B \frac{1+\varepsilon}{2} K_h \right] x(t) \\ &\quad + \epsilon_1 \left(\bar{u}(t) - \frac{1+\varepsilon}{2} u(t) \right)^{\mathrm{T}} \left(\bar{u}(t) - \frac{1+\varepsilon}{2} u(t) \right) + \epsilon_1^{-1} x^{\mathrm{T}}(t) P B B^{\mathrm{T}} P x(t) \\ &\leq x^{\mathrm{T}}(t) \begin{bmatrix} A_h^{\mathrm{T}} P + P A_h + \left(B \frac{1+\varepsilon}{2} K_h \right)^{\mathrm{T}} P + P B \frac{1+\varepsilon}{2} K_h \\ + \epsilon_1 \left(\frac{1-\varepsilon}{2} \right)^2 K_h^{\mathrm{T}} K_h + \epsilon_1^{-1} P B B^{\mathrm{T}} P + \epsilon_2 E_h^{\mathrm{T}} E_h + \epsilon_2^{-1} P H H^{\mathrm{T}} P \end{bmatrix} x(t). \end{aligned}$$

$$x^{\mathrm{T}}(t) \begin{bmatrix} A_h^{\mathrm{T}} P + P A_h + \left(B \frac{1+\varepsilon}{2} K_h \right)^{\mathrm{T}} P + P B \frac{1+\varepsilon}{2} K_h \\ + \epsilon_1 \left(\frac{1-\varepsilon}{2} \right)^2 K_h^{\mathrm{T}} K_h + \epsilon_1^{-1} P B B^{\mathrm{T}} P + \epsilon_2 E_h^{\mathrm{T}} E_h + \epsilon_2^{-1} P H H^{\mathrm{T}} P \end{bmatrix} x(t) \leq -2\alpha x^{\mathrm{T}}(t) P x(t). \tag{24}$$

$$\Pi = \begin{bmatrix} A_h^{\mathrm{T}} P + P A_h + \left(B \frac{1+\varepsilon}{2} K_h \right)^{\mathrm{T}} P + P B \frac{1+\varepsilon}{2} K_h \\ + \epsilon_1 \left(\frac{1-\varepsilon}{2} \right)^2 K_h^{\mathrm{T}} K_h + \epsilon_1^{-1} P B B^{\mathrm{T}} P + \epsilon_2 E_h^{\mathrm{T}} E_h + \epsilon_2^{-1} P H H^{\mathrm{T}} P + 2\alpha P \end{bmatrix} < 0 \tag{25}$$

$$\Sigma = \begin{bmatrix} Q A_h^{\mathrm{T}} + A_h Q + \frac{1+\varepsilon}{2} Y_h^{\mathrm{T}} B^{\mathrm{T}} + \frac{1+\varepsilon}{2} B Y_h \\ + \epsilon_1 \left(\frac{1-\varepsilon}{2} \right)^2 Y_h^{\mathrm{T}} Y_h + \epsilon_1^{-1} B B^{\mathrm{T}} + \epsilon_2 Q E_h^{\mathrm{T}} E_h Q + \epsilon_2^{-1} H H^{\mathrm{T}} + 2\alpha Q \end{bmatrix} < 0. \tag{26}$$

$$\Theta = \begin{bmatrix} A_h^{\mathrm{T}} + A_h Q + \frac{1+\varepsilon}{2} \left[Y_h^{\mathrm{T}} B^{\mathrm{T}} + B Y_h \right] + \epsilon_1^{-1} B B^{\mathrm{T}} + \epsilon_2^{-1} H H^{\mathrm{T}} + 2\alpha Q & Y_h^{\mathrm{T}} & Q E_h^{\mathrm{T}} \\ * & -\epsilon_1^{-1} \left(\frac{2}{1-\varepsilon} \right)^2 I & 0 \\ * & * & -\epsilon_2^{-1} I \end{bmatrix} < 0. \tag{27}$$

TABLE I
PARAMETER VALUES OF THE AMB MODEL

Symbol	N	m	A_g	$v_{\max}$
Meaning	number of turns in coil	effective mass rotor	electromagnet pole area	maximum voltage
Unit	#	kg	mm	V
Value	321	4.5	137	10

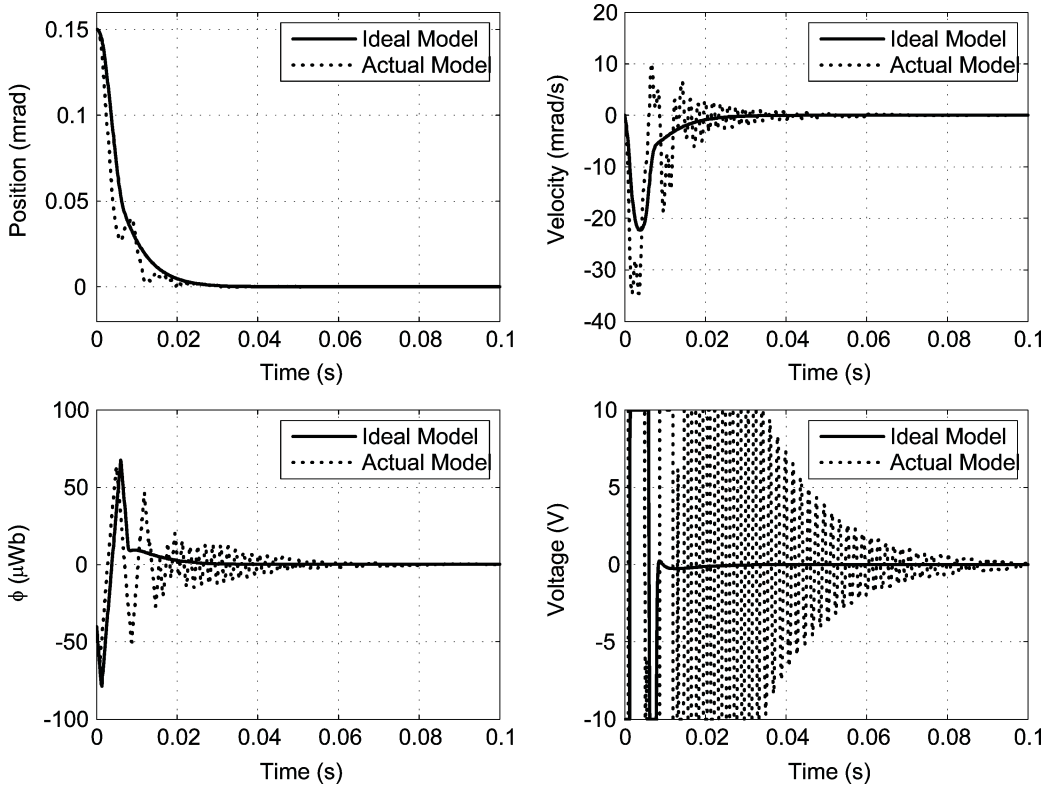

Fig. 2. Comparison of state trajectories and control voltages for 'ideal' and 'actual' AMB models with $\phi_1(0) = 10\ \mu$Wb and $\phi_1(0) = 50\ \mu$Wb .

model includes flux leakage, magnetic-material saturation, flexible modes, voltage saturation, and coil resistance. It has been shown that this mathematical model represents the actual AMB test rig very accurately [7], [10], and hence, it can be used to validate the control design under realistic conditions. In this paper, we call such a model the "actual" AMB model to distinguish it from the "ideal" model (10) (with coil resistance, flux leakage, magnetic-material saturation, flexible modes neglected). The basic bearing parameter values are listed in Table I

As in [3] and [4], the bias flux in the simulations is chosen as $\Phi_0 = 10\ \mu$Wb, and the voltage-saturation level is chosen as $v_{\max} = 10$ V. The initial conditions are set to $z(0) = 0.15$ mm (or mrad), $\dot{z}(0) = 0$ mm/s (or mrad/s), $\phi_1(0) = 10\ \mu$Wb, and $\phi_2(0) = 50\ \mu$Wb. The earlier control flux values are for the total flux in the magnetic-levitation system which includes gap flux and flux leakage.

In this paper, the control input is limited as $u_{\lim} = 10$ V, and the generalized control flux is limited to $200\ \mu$Wb such that the bounds of the nonlinear function (11) is given as $f_{\min} = 0$ and $f_{\max} = 200$. For simplicity of presentation, we consider the uncertainties of bias flux and initial conditions of control flux and define the uncertain matrices as $\Delta A_1 = \Delta A_2 = HFE$, where the matrices $H = [0, 1, 0]^{\mathrm{T}}$ and $E = [0, 0, 0.5\beta_0]$, which may allow 50% variation of parameter β_0. To design a high-gain controller and to yield a fast convergence possible for the state $z(t)$, the controller design parameters are selected as $\varepsilon = 0.5$, $\rho = 0.3$, and $\alpha = 128$ after several trials. Note that we may choose a larger value for α to get a faster convergence rate for the "ideal" model because it does not include magnetic-material saturation, and the flux-saturation level can be increased to enable the controller to work well. However, when the designed controller is applied to the "actual" model, it will not work due to the magnetic-material saturation. Therefore, the parameter α cannot be chosen too large. Using the controller design approach presented in the previous section, we obtain the controller gains as

$$K_1 = [\,-2.6408 \times 10^6 \quad -2.0748 \times 10^4 \quad -2.0090 \times 10^6\,]$$
$$K_2 = [\,-2.6988 \times 10^6 \quad -2.0979 \times 10^4 \quad -2.6057 \times 10^6\,].$$

The simulation program is realized by MATLAB/Simulink, and the simulation results for the system states $z(t)$, $\dot{z}(t)$, and $\phi(t)$ and for the control voltage $v(t)$ are shown in Fig. 2, where the simulation results of the "ideal" AMB model are compared with the "actual" (high fidelity) AMB model. It is shown in Fig. 2 that the position responses "quickly" converge to zero

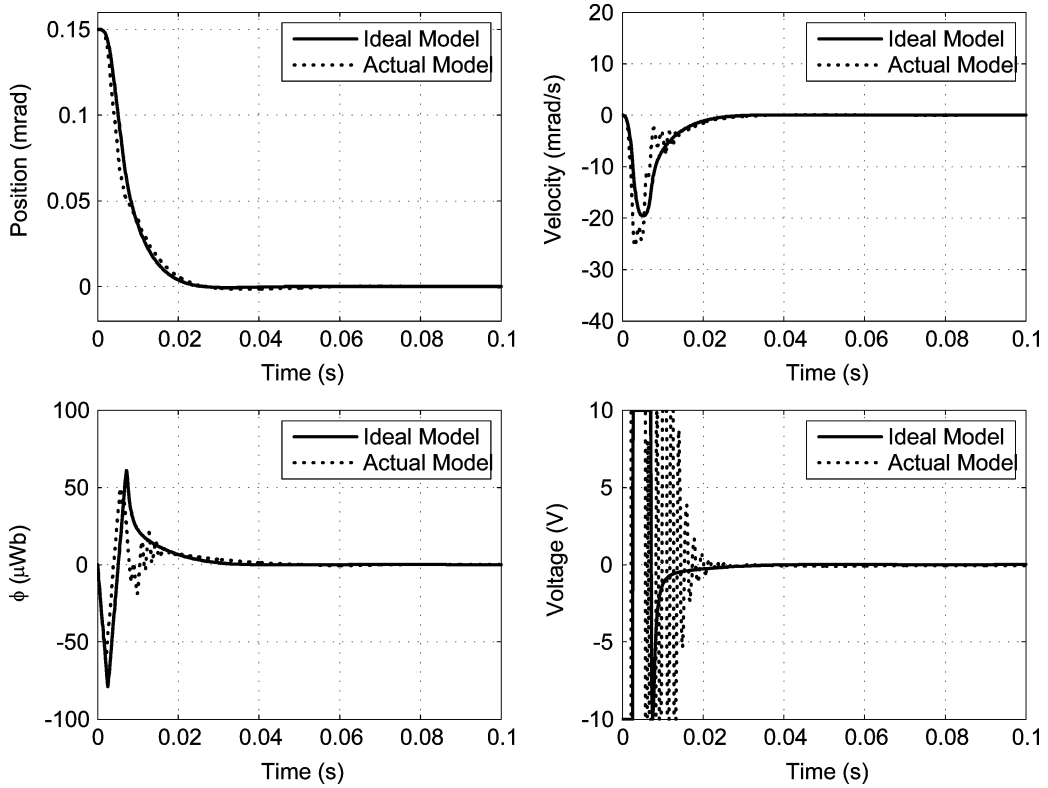

Fig. 3. Comparison of state trajectories and control voltages for 'ideal' and 'actual' AMB models with $\phi_1(0) = 0\ \mu$Wb and $\phi_2(0) = 0\ \mu$Wb .

for two models and the position response of the control implementation on the "actual" AMB model is "close" to the position response of the control action on the "ideal" AMB model which is used for the controller design. When compared with the simulations of the controllers from [3] and [4], our controller yields similar closed-loop performance with respect to the position settling time.

Now, consider one case that we change the initial conditions for control flux as $\phi_1(0) = 0\ \mu$Wb and $\phi_2(0) = 0\ \mu$Wb, which are different from the initial conditions used for the controller design, and keep the other conditions unchanged. Thus, the parameter β_0 is reduced to half of the value that is used to design the controller. In this case, the same controller as designed earlier is applied to both the "ideal" and the "actual" models. The simulation results are shown in Fig. 3. It is shown in Fig. 3 that the position responses for two models all converge to zero "quickly." Compared the position response of the "ideal" AMB model with that shown in Fig. 2, it is shown that the two position responses are similar regardless of the variation on the parameter β_0. It shows that the designed controller appears to be robust to uncertainties in the AMB model parameters.

VI. Conclusion

In this paper, we present a robust fuzzy state-feedback control strategy for a recently developed low-bias AMB model subject to control-voltage saturation. Using the idea of "sector nonlinearity," the nonlinear uncertain AMB model is represented by a T-S fuzzy model in a defined region. By means of the PDC scheme, a fuzzy state-feedback controller is designed to stabilize the obtained T-S fuzzy model with a given decay rate. At the same time, the control-voltage constraint is involved in the controller design process. The sufficient conditions for designing such a controller are expressed by linear matrix inequalities. Numerical simulations are used to validate the effectiveness of the designed controller.

Acknowledgment

The authors would like to thank the anonymous reviewers for their invaluable comments.

References

[1] P. Tsiotras and B. C. Wilson, "Zero and low-bias control designs for active magnetic bearings," *IEEE Trans. Control Syst. Technol.*, vol. 11, no. 6, pp. 889–904, Nov. 2003.

[2] B. C. Wilson, "Control designs for low-loss active magnetic bearings: Theory and implementation," Ph.D. dissertation, School Elect. Comput. Eng., Georgia Inst. Technol., Atlanta, 2004.

[3] P. Tsiotras and M. Arcak, "Low-bias control of AMB subject to voltage saturation: State-feedback and observer designs," *IEEE Trans. Control Syst. Technol.*, vol. 13, no. 2, pp. 262–273, Mar. 2005.

[4] F. Mazenc, M. S. de Queiroz, M. Malisoff, and F. Gao, "Further results on active magnetic bearing control with input saturation," *IEEE Trans. Control Syst. Technol.*, vol. 14, no. 5, pp. 914–919, Sep. 2006.

[5] M. N. Sahinkaya and A. E. Hartavi, "Variable bias current in magnetic bearings for energy optimization," *IEEE Trans. Magn.*, vol. 43, no. 3, pp. 1052–1060, Mar. 2007.

[6] K. Tanaka and H. O. Wang, *Fuzzy Control Systems Design and Analysis: A Linear Matrix Inequality Approach*. New York: Wiley, 2001.

[7] J. D. Lindlau and C. R. Knospe, "Feedback linearization of an active magnetic bearing with voltage control," *IEEE Trans. Control Syst. Technol.*, vol. 10, no. 1, pp. 21–31, Jan. 2002.

[8] Y.-Y. Cao and Z. Lin, "Robust stability analysis and fuzzy-scheduling control for nonlinear systems subject to actuator saturation," *IEEE Trans. Fuzzy Syst.*, vol. 11, no. l, pp. 57–67, Feb. 2003.

[9] J. H. Kim and F. Jabbari, "Actuator saturation and control design for buildings under seismic excitation," *J. Eng. Mech.*, vol. 128, no. 4, pp. 403–412, Apr. 2002.

[10] C. Knospe, "The nonlinear control benchmark experiment," in *Proc. Amer. Control Conf.*, Chicago, IL, 2000, pp. 2134–2138.